# NQNN: Noise-aware Quantum Neural Networks for Medical Image Classification

Maqsudur Rahman[1,2][0009−0007−5240−0662] and Jun Zhuang[1][0000−0002−7142−2193]

[1] Boise State University, Boise, ID 837206, USA.
[2] Comilla University, Cumilla 3500, Bangladesh.
mrrajon@cou.ac.bd

**Abstract.** Noisy labels in high-dimensional, and multiclass medical image datasets pose a significant challenge for machine learning models. While hybrid quantum-classical architectures, such as quantum neural networks (QNNs), have shown promise in medical imaging, their robustness under noisy label conditions remains largely unexplored. To address this gap, we propose a Noise-aware Quantum Neural Network (NQNN), integrating Fourier Attenuation, Reweight Estimation, and Adaptive Pooling to enhance feature extraction and classification robustness. Fourier Attenuation filters high-frequency noise, Reweight Estimation prioritizes cleaner labels based on uncertainty, and Adaptive Pooling dynamically refines feature aggregation. We evaluate NQNN on six benchmark medical datasets (PathMNIST, BloodMNIST, OrganAMNIST, OrganCMNIST, OCTMNIST, and DermaMNIST) across noise ratios (10%, 30%, and 50%) and classification configurations (binary, four-class, and full multiclass). Comparative benchmarks against five QNN-based and two deep-learning baselines demonstrate NQNN's superior performance, such as achieving 80.25% accuracy on organCMNIST at 10% noise and maintaining strong performance at higher noise ratios. Our ablation studies validate the effectiveness of each noise-handling mechanism, highlighting their complementary contributions to noise robustness. By bridging quantum advancements with real-world medical diagnostics, NQNN establishes a new benchmark for noise-resilient medical image classification, offering a scalable and adaptive quantum-classical learning framework.

**Keywords:** Medical Image Classification · Quantum Neural Networks (QNNs) · Noisy Label Learning.

## 1 Introduction

Medical image datasets heavily rely on expert annotations, yet these annotations are inherently prone to label noise due to subjectivity error (10; 25). Thus, noisy labels can significantly degrade model performance, particularly in high-dimensional and multiclass datasets. While deep-learning approaches, such as label correction techniques and robust loss functions, have demonstrated efficacy in mitigating these shortcomings (17; 21), they often depend on clean validation sets or the assumption of specific noise distributions, which is limited in real-world settings. Quantum Neural Networks (QNNs), which integrate quantum circuits with neural network layers, have emerged as a promising paradigm for multiclass medical image classification due to their potential for high-dimensional feature representation and quantum parallelism (14; 12; 26). However, their applicability under noisy-label conditions—where annotations may be incorrect or inconsistent—remains largely unexplored. In particular, no prior work has systematically evaluated the noise robustness of QNNs or adapted them to address mislabeled data in multiclass clinical imaging scenarios. To address this gap, we introduce a hybrid quantum-classical framework, namely Noise-aware Quantum Neural Network (NQNN), specifically designed to improve robustness under noisy label conditions. Our motivation stems from the need to ensure model reliability when medical image annotations are flawed—an issue often encountered in practice. NQNN integrates three complementary mechanisms—Fourier Attenuation, Reweight Estimation, and Adaptive Pooling—within a Variational Quantum Circuit (VQC). Fourier Attenuation filters high-frequency noise through quantum Fourier transforms and controlled phase rotations, enhancing feature clarity (7). Reweight Estimation prioritizes cleaner labels by adjusting sample importance based on noise levels (9). Adaptive Pooling refines feature aggregation by dynamically adjusting quantum operations based on noise distribution, ensuring robust feature retention (19; 4). We conduct extensive experiments on six benchmark datasets from MedMNISTv2 to validate the effectiveness of NQNN under varying levels of symmetric label noise (10%, 30%, and 50%) and across multiple classification configurations (binary, four-class, and full multiclass). Our experiments also include evaluations on clean datasets to ensure that noise-resilient mechanisms do not compromise performance in standard settings.

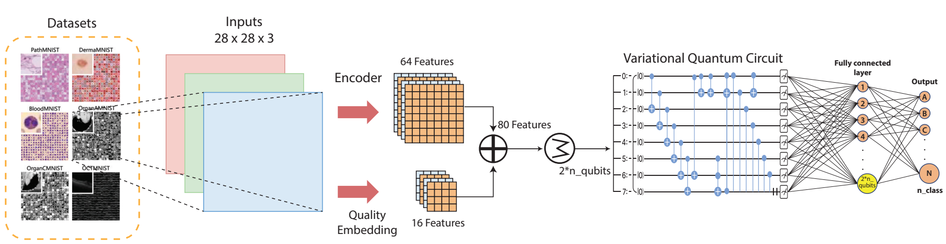


Fig. 1: Our framework consists of **feature extraction** using an **Encoder** and a **Quality Embedding Network**, followed by **Variational Quantum Circuit** processing with three noise-resilient mechanisms for ensuring robust multiclass classification under clean and noisy labels.

## 2 Proposed Noise-Aware Quantum Neural Networks

We propose a noise-aware quantum-classical framework, NQNN, for multiclass medical image classification where label noise is prevalent. As shown in Fig. 1, the architecture integrates a hybrid classical-quantum pipeline with three complementary noise-resilient mechanisms embedded into a Variational Quantum Circuit (VQC): Fourier Attenuation, Reweight Estimation, and Adaptive Pooling. These modules address distinct noise dimensions—frequency, uncertainty, and spatial variability. The classical frontend consists of an **Encoder** that extracts 64-dimensional spatial features from medical images and a **Quality Embedding Network** that outputs a 16-dimensional uncertainty-aware representation. To capture label noise, the network computes two types of uncertainty—disagreement uncertainty $U_d$ and single-target (entropy) uncertainty $U_s$—based on the predicted class probabilities $p_c$ from the softmax output.

$$U_d(x_i) = 1 - \sum_{c=1}^{C} p_c^2, \quad U_s(x_i) = -\sum_{c=1}^{C} p_c \log p_c. \tag{1}$$

The outputs from both modules are concatenated into an 80-dimensional feature vector, which serves as the input to the VQC for quantum processing. The **Variational Quantum Circuit** (Fig. 2) encodes the 80-dimensional vector into quantum states using parameterized Rx and Rz gates. Entanglement is introduced through CNOT operations across qubit pairs, enabling complex correlations to enhance feature representation. **Fourier Attenuation** suppresses high-frequency label noise by operating in the frequency domain. The input feature signal $f(x)$ is transformed via the Fourier Transform (Eq. 2):

$$F(u) = \int_{-\infty}^{\infty} f(x) e^{-2\pi i u x} dx, \tag{2}$$

and filtered by a low-pass mask, where $F'(u) = F(u)$ if $|u| \leq u_c$, and 0 otherwise, and then reconstructed back to the spatial domain via inverse transform (Eq. 3):

$$f'(x) = \int_{-\infty}^{\infty} F'(u) e^{2\pi i u x} du. \tag{3}$$

**Reweight Estimation** assigns sample-wise importance weights by combining both uncertainty measures. These weights modulate the rotation angles of quantum gates, emphasizing cleaner samples during training:

$$w_i = 1 - (U_d(x_i) + U_s(x_i)). \tag{4}$$

**Adaptive Pooling** preserves key spatial patterns by adjusting pooling scales according to the input and output dimensions, mitigating the influence of noisy spatial features:

$$s_h = \frac{\text{Input Height}}{\text{Output Height}}, \quad s_w = \frac{\text{Input Width}}{\text{Output Width}}. \tag{5}$$

Finally, the quantum circuit outputs are measured using Pauli-Z observables. The collapsed quantum states are passed to a fully connected layer, producing class predictions. This integrated architecture enables robust learning from noisy-labeled, low-resolution medical images while remaining compatible with near-term quantum simulation constraints.

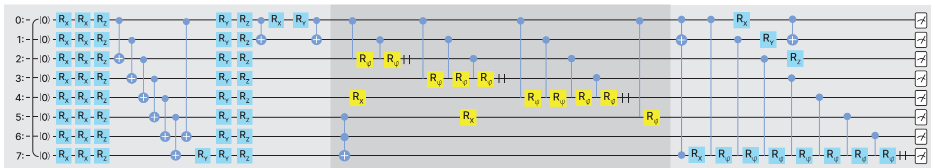

Fig. 2: A single block of the Variational Quantum Circuit in the NQNN framework. This block represents **data encoding layers** using $R_x$ and $R_z$ gates, **entanglement operations** via CNOT gates, and **trainable quantum layers** with parameterized rotations $(R_x, R_y, R_z)$, **controlled phase rotations and Hadamard gates** and dynamically adjust quantum rotations to suppress high-frequency noise and enhance feature aggregation under noisy label conditions.

## 3 Experiments

In this section, we introduce our experimental settings and discuss the results.
**Datasets:** We evaluate NQNN on six medical image datasets from MedMNISTv2 (23), chosen for their diversity, clinical relevance, and compatibility with quantum simulation. All datasets are standardized to $28 \times 28$ **resolution** and evaluated under **10%, 30%, and 50% symmetric label noise** by randomly flipping class labels. **PathMNIST(D1)** (107,180 samples, 9 classes) includes colorectal cancer histology patches. **BloodMNIST(D2)** (17,092 samples, 8 classes) features visually similar blood cells. **OrganAMNIST(D3)** (58,218 samples, 11 classes) and **OrganCMNIST(D4)** (24,292 samples, 11 classes) contain abdominal CT slices for organ classification. **OCTMNIST(D5)** (109,309 samples, 4 classes) differentiates retinal diseases via OCT. **DermaMNIST(D6)** (10,015 samples, 7 classes) includes dermatoscopic images of skin conditions. These datasets present challenging multiclass tasks under structured label noise, ideal for assessing robustness in simulation-constrained quantum models.
**Hyperparameter Settings and Evaluation:** All models, including NQNN and baselines, were trained with the Adam optimizer (0.001 learning rate, 128 batch size) and cross-entropy loss for up to 30 epochs with early stopping on validation loss. We use accuracy (ACC) as the main evaluation metric for classification. Experiments were conducted using the Pennylane simulator with GPU acceleration (Ubuntu 20.04, Python 3.9, TensorFlow 2.6, PyTorch 1.10, Pennylane 0.25). For reproducibility, the full implementation and supplementary materials are available here.

Table 1: Classification Performance of NQNN on Clean Medical Datasets Under Different Number of Classes $|C|$ Settings.

| **Data** | $\lvert C\rvert$ | **QCNN** | **QTNet** | **HQNet** | **QCCNet** | **A-HQCNN** | **NQNN** |
|---|---|---|---|---|---|---|---|
| **D1** | C2 | 69.79% | 47.13% | 47.95% | 52.25% | 50.00% | **81.59%** |
| | C4 | 62.92% | 25.33% | 23.28% | 23.38% | 24.62% | **76.15%** |
| | All | 61.65% | 13.95% | 11.63% | 11.42% | 12.66% | **75.21%** |
| **D2** | C2 | 65.70% | 48.84% | 50.26% | 49.58% | 54.64% | **86.80%** |
| | C4 | 63.53% | 25.89% | 24.59% | 25.06% | 43.47% | **76.41%** |
| | All | 62.48% | 12.32% | 12.30% | 12.69% | 20.17% | **73.73%** |
| **D3** | C2 | 69.21% | 50.07% | 50.81% | 50.67% | 50.13% | **73.73%** |
| | C4 | 65.44% | 25.55% | 24.49% | 24.54% | 24.70% | **84.38%** |
| | All | 61.76% | 12.52% | 12.36% | 12.57% | 12.01% | **81.43%** |
| **D4** | C2 | 69.43% | 49.33% | 49.84% | 49.84% | 77.88% | **84.50%** |
| | C4 | 67.78% | 24.37% | 23.53% | 23.58% | 44.42% | **82.73%** |
| | All | 63.01% | 13.18% | 11.95% | 12.92% | 21.66% | **79.92%** |
| **D5** | C2 | 51.27% | 50.60% | 49.16% | 48.99% | 49.66% | **69.05%** |
| | C4 | 45.08% | 35.79% | 34.90% | 35.20% | 34.77% | **64.86%** |
| | All | 38.47% | 25.79% | 24.90% | 25.20% | 24.77% | **59.05%** |
| **D6** | C2 | 50.38% | 47.33% | 55.73% | 48.85% | 40.00% | **89.61%** |
| | C4 | 48.47% | 30.65% | 35.61% | 29.56% | 35.44% | **83.74%** |
| | All | 41.47% | 20.65% | 32.61% | 21.56% | 25.44% | **82.67%** |

**Competing Methods:** We benchmark NQNN against five quantum and two classical baselines, selected for their methodological relevance to quantum or noise-resilient medical image classification. Our goal is not to critique or diminish prior work, but to contextualize our noise-resilient layers within existing quantum and classical frameworks. As no existing QNNs are explicitly designed for multiclass noisy-label scenarios, we faithfully reproduced these baselines from their original descriptions to evaluate their generalization performance under controlled label noise. **QCNN** (Quantum Convolutional Neural Network) (3) introduced quantum convolution and pooling layers for efficient quantum feature extraction. **QTNet** (Quantum Transfer Learning Network) (5) combined classical ResNet18 with quantum variational circuits for multiclass classification scalability. **HQNet** (Hybrid Quantum Neural Network) (16) integrated classical CNNs with quantum convolutional layers for feature learning. **QCCNet** (Quantum Circuit-based Convolutional Network) (24) proposed a structured quantum circuit architecture optimized for computational efficiency. **A-HQCNN** (Adaptive Hybrid Quantum CNN) (1) utilized parameterized quantum convolutional layers with adaptive optimizers for improved convergence. These quantum models were originally designed and validated under clean-label scenarios, and we recognize the value of their contributions in advancing hybrid and quantum learning. In our study, we evaluated their performance under synthetic label noise to assess the generalizability of such frameworks, not to suggest limitations in their original context. We also include two classical baselines designed specifically for noisy-label settings. **DUE-Net** (Dual-Uncertainty Estimation Network) (9) leveraged disagreement and entropy-based uncertainty for reweighting with Monte Carlo Dropout. **RWNet** (6) applied noise transition matrices and reweighting techniques for label correction. These models provided strong baselines for classical robustness under noisy annotations. All baseline implementations were either adapted from original code (where available) or faithfully re-implemented following their respective publications, ensuring consistent preprocessing, training, and evaluation pipelines across all datasets. Our comparison highlights the effectiveness of integrating noise-resilient layers into QNNs while respecting the foundational contributions of prior methods.

**Results and Discussion:** We present and discuss the performance of NQNN under three settings: (i) multiclass classification on clean datasets, (ii) noisy label classification, and (iii) an ablation study assessing noise-handling mechanisms. The results highlight NQNN's robustness, scalability, and effectiveness in handling multiclass medical image classification under noisy labels.

**(i) Classification Performance on Clean Datasets:** We evaluate NQNN against five QNN-based baselines on six datasets under three settings: binary (C2), four-class (C4), and full multiclass, in Tab. 1. NQNN consistently outperforms all baselines across datasets. For BloodMNIST, NQNN achieved 86.80% in C2, 76.41% in C4, and 73.73% in All, significantly outperforming QCNN (65.70%, 63.53%, 62.48%). PathMNIST exhibited similar trends due to the lack of dedicated noise-handling mechanisms and conventional label correction methods in baseline models. In more complex datasets like OrganAMNIST and OrganCMNIST, NQNN outperforms all the baselines in every setting for noise-resilient feature extraction mechanisms. Consequently, the results presented in Tab. 1 collectively demonstrate that our three proposed mechanisms significantly enhance NQNN, making it a highly scalable and noise-resilient model for medical image classification, outperforming all baseline models.

**(ii) Noisy Label Classification Under Different Noise Ratios:** We evaluate NQNN across noise levels (10%, 30%, 50%) on all datasets, with results in Tab. 2. NQNN consistently outperforms QNN baselines and remains competitive with deep learning models, showing greater robustness as noise increases. In PathMNIST, NQNN achieved 71.32% at 10% noise, surpassing all QNN baselines and closely approaching DUE-Net (80.23%). At 30% and 50%, NQNN maintained 63.49% and 58.02%, outperforming QNN baselines that exhibited sharper declines, while deep learning models struggled with label correction failures. BloodMNIST showed a similar trend, with NQNN reaching 70.39%, 64.78%, and 61.93%, whereas RWNet and DUE-Net experienced steep accuracy drops at higher noise levels. In OrganAMNIST, NQNN demonstrated strong noise resilience, achieving 80.32% at 10% noise, outperforming most QNN baselines and RWNet (44.83%). In OCTMNIST, NQNN reached 78.32% at 10% noise, sustaining 59.88% and 61.61% at higher noise levels, where baseline models struggled

Table 2: Comparison between NQNN and Baseline Models on Multi-class Classification Under Different Noise Ratios, $nr$.

| **nr** | **Models** | **D1** | **D2** | **D3** | **D4** | **D5** | **D6** |
|---|---|---|---|---|---|---|---|
| 10% | QCNN (3) | 65.97% | 64.22% | 63.82% | 63.07% | 24.53% | 54.28% |
| | QTNet (5) | 12.22% | 13.33% | 12.29% | 9.39% | 26.46% | 17.57% |
| | HQNet (16) | 12.83% | 13.80% | 14.25% | 9.75% | 25.31% | 16.43% |
| | QCCNet (24) | 13.43% | 13.89% | 13.98% | 9.66% | 26.84% | 22.86% |
| | A-HQCNN (1) | 25.95% | 23.04% | 15.18% | 14.07% | 27.61% | 13.66% |
| | DUE-Net (9) | **80.23%** | **82.30%** | 29.03% | **86.93%** | 52.37% | 41.61% |
| | RWNet (6) | 76.15% | 79.67% | 44.83% | 83.46% | 50.01% | 22.98% |
| | **NQNN** | 71.32% | 70.39% | **80.32%** | 78.32% | **55.33%** | **80.25%** |
| 30% | QCNN (3) | 58.05% | 53.36% | 52.34% | 53.52% | 21.31% | 46.43% |
| | QTNet (5) | 10.76% | 12.50% | 11.80% | 8.50% | 19.69% | 15.14% |
| | HQNet (16) | 10.57% | 13.86% | 13.06% | 8.24% | 24.22% | 15.57% |
| | QCCNet (24) | 13.19% | 11.09% | 10.55% | 9.60% | 24.25% | 20.14% |
| | A-HQCNN (1) | 24.26% | 22.97% | 14.89% | 10.89% | 25.34% | 11.06% |
| | DUE-Net (9) | 59.05% | 64.64% | 28.86% | **68.65%** | 45.45% | 27.95% |
| | RWNet (6) | 60.13% | 54.19% | 35.00% | 64.99% | 44.29% | 22.36% |
| | **NQNN** | **63.49%** | **64.78%** | **73.88%** | 59.88% | **46.55%** | **71.01%** |
| 50% | QCNN (3) | 46.32% | 46.59% | 44.04% | 42.46% | 14.69% | 42.14% |
| | QTNet (5) | 8.18% | 13.07% | 12.03% | 9.60% | 10.00% | 13.00% |
| | HQNet (16) | 10.35% | 10.52% | 13.36% | 8.15% | 23.91% | 13.00% |
| | QCCNet (24) | 11.53% | 11.20% | 12.50% | 9.60% | 22.97% | 17.00% |
| | A-HQCNN (1) | 15.23% | 22.33% | 12.60% | 10.26% | 24.14% | 11.16% |
| | DUE-Net (9) | 48.35% | 49.77% | 23.92% | 48.82% | 40.62% | 24.22% |
| | RWNet (6) | 44.55% | 43.90% | 28.28% | 46.90% | 40.70% | 19.25% |
| | **NQNN** | **58.02%** | **61.93%** | **61.69%** | **61.61%** | **41.71%** | **66.14%** |

due to dataset complexity. While quantum models face dataset size constraints across all datasets, NQNN maintained stability under increasing noise, demonstrating the effectiveness of noise-resilient mechanisms in mitigating label noise.

**(iii) Ablation Study on Noise-resilient Mechanisms:** We assess the contributions of Reweight Estimation (A), Fourier Attenuation (B), and Adaptive Pooling (C) in Tab. 3. Fourier Attenuation performed best individually, particularly in high inter-class similarity datasets like OrganCMNIST (73.27% at 10%). However, the combination of A+B achieved more robust performance, reaching 66.78% on BloodMNIST at 10% noise and maintaining 57.32% on OrganAMNIST at 50% noise. The A+B+C combination (NQNN) consistently outperformed all configurations, demonstrating that integrating noise-aware weighting, frequency filtering, and spatial consistency mechanisms enhances scalability and robustness in noisy medical image classification.

Table 3: Ablation Study: Evaluating Individual and Combined Noise-Resilient Feature Extraction Mechanisms in NQNN under Different Noise Ratios, $nr$.

| **Dataset** | **nr** | **A** | **B** | **C** | **A+B** | **B+C** | **A+C** | **A+B+C** |
|---|---|---|---|---|---|---|---|---|
| **D1** | 10% | 51.12% | 55.51% | 31.35% | 61.04% | 54.10% | 51.92% | **71.32%** |
| | 30% | 37.10% | 41.26% | 25.35% | 53.39% | 40.99% | 27.10% | **63.49%** |
| | 50% | 31.20% | 35.21% | 21.26% | 44.04% | 35.99% | 31.20% | **58.02%** |
| **D2** | 10% | 58.09% | 61.05% | 48.09% | 66.78% | 59.25% | 58.09% | **70.39%** |
| | 30% | 56.15% | 56.59% | 43.22% | 63.97% | 54.70% | 56.15% | **64.78%** |
| | 50% | 45.59% | 50.45% | 33.22% | 51.22% | 49.45% | 45.59% | **61.93%** |
| **D3** | 10% | 51.16% | 61.46% | 41.49% | 71.55% | 61.06% | 52.16% | **80.32%** |
| | 30% | 43.65% | 51.46% | 33.74% | 63.01% | 52.28% | 46.65% | **73.88%** |
| | 50% | 38.65% | 42.43% | 32.46% | 57.32% | 46.01% | 40.65% | **61.69%** |
| **D4** | 10% | 61.19% | 71.21% | 50.81% | 73.27% | 72.21% | 62.19% | **78.32%** |
| | 30% | 52.91% | 57.99% | 42.32% | 58.00% | 53.41% | 53.91% | **59.88%** |
| | 50% | 38.28% | 56.74% | 29.32% | 55.79% | 47.07% | 39.28% | **61.61%** |
| **D5** | 10% | 42.52% | 45.38% | 32.47% | 48.25% | 47.52% | 42.52% | **55.33%** |
| | 30% | 37.45% | 39.24% | 27.96% | 45.55% | 42.99% | 37.45% | **46.55%** |
| | 50% | 33.61% | 34.98% | 25.23% | 34.92% | 39.90% | 33.61% | **41.71%** |
| **D6** | 10% | 24.77% | 24.28% | 17.32% | 65.46% | 53.82% | 54.77% | **80.25%** |
| | 30% | 22.84% | 21.11% | 12.98% | 52.98% | 51.56% | 42.84% | **71.01%** |
| | 50% | 21.73% | 19.87% | 10.66% | 43.04% | 47.82% | 31.73% | **66.14%** |

## 4 Related Works

Several studies have explored noise-resilient learning across classical and quantum settings. In the quantum domain, Mathur et al. (15) introduced Quantum Orthogonal Neural Networks (QOrthoNN) to prevent gradient vanishing, while Trochun et al. (20) validated hybrid quantum models under noisy label scenarios. Xue et al. (22) proposed collaborative co-training with label filters for robust classification, and Khanal et al. (11) showed Vision Transformers (ViTs) outperform CNNs in noisy settings via self-supervised learning. In the classical domain, Veit et al. (21) proposed a multi-task label-cleaning network to handle large-scale noise. Lee et al. (13) introduced CleanNet for scalable noise reduction using transfer learning, and Gao et al. (8) designed Deep Label Distribution Learning (DLDL) to represent ambiguity through distributions. Other contributions include Rank Pruning (17) for eliminating low-confidence samples, ensemble-based soft label generation (18), and knowledge distillation for label denoising (2). These works inform our noise-handling mechanisms, but none embed them directly into quantum circuits. NQNN builds on these ideas by extending noise-resilient learning to Variational Quantum Circuits, where label noise robustness remains underexplored.

## 5 Conclusion and Future Work

This study introduces NQNN, a quantum-classical framework for multiclass medical image classification, integrating Fourier Attenuation, Reweight Estimation, and Adaptive Pooling to enhance robustness under noisy labels. NQNN is the first framework to embed noise-resilient mechanisms directly within a Variational Quantum Circuit (VQC), addressing noisy-label robustness in multiclass medical imaging—a gap unaddressed in prior QNN studies. Extensive experiments on six benchmark datasets across varying settings and noise ratios (10%, 30%, 50%) demonstrate that our framework achieves superiority over all baselines. The VQC enables structured noise mitigation while remaining feasible under current simulation constraints via shallow-depth circuits and low qubit count. In the future, we will focus on optimizing circuit depth for scalability on real quantum hardware and extending NQNN to handle structured and asymmetric label noise for broader medical AI applications.

**Disclosure of Interests.** The authors declare no competing interests. All contributions were made for academic purposes.

# Bibliography


[1] Ajlouni, N., Özyavaş, A., Takaoğlu, M., Takaoğlu, F., Ajlouni, F.: Medical image diagnosis based on adaptive hybrid quantum cnn. BMC Medical Imaging **23**(1), 126 (2023)

[2] Aliev, V., Ostyakov, P., Suvorov, R., Sterkin, G., Logacheva, E., Khomenko, O., Nikolenko, S.: Label denoising with large ensembles of heterogeneous neural networks. In: Proc. of the 2nd Workshop on YouTube-8M Large-Scale Video Understanding (2018)

[3] Bokhan, D., Mastiukova, A.S., Boev, A.S., Trubnikov, D.N., Fedorov, A.K.: Multiclass classification using quantum convolutional neural networks with hybrid quantum-classical learning. Frontiers in Physics **10**, 1069985 (2022)

[4] Damian, A., Warmuth, M.K., Zhang, L., Chen, B., Li, F.: Analysis of classifiers robust to noisy labels. Proceedings of the 36th International Conference on Machine Learning **97**, 1500–1509 (2019), `http://proceedings.mlr.press/v97/damian19a.html`

[5] Dhara, B., Agrawal, M., Roy, S.D.: Multi-class classification using quantum transfer learning. Quantum Information Processing **23**(2), 34 (2024)

[6] Díaz, A., Steele, D.: Analysis of classifiers robust to noisy labels. arXiv preprint arXiv:2106.00274 (2021)

[7] Englesson, E., Azizpour, H.: Robust classification via regression for learning with noisy labels. In: ICLR 2024-The Twelfth International Conference on Learning Representations, Messe Wien Exhibition and Congress Center, Vienna, Austria, May 7-11t, 2024 (2024)

[8] Gao, B.B., Xing, C., Xie, C.W., Wu, J., Geng, X.: Deep label distribution learning with label ambiguity. IEEE Transactions on Image Processing **26**(6), 2825–2838 (2017)

[9] Ju, L., Wang, X., Wang, L., Mahapatra, D., Zhao, X., Zhou, Q., Liu, T., Ge, Z.: Improving medical images classification with label noise using dual-uncertainty estimation. IEEE transactions on medical imaging **41**(6), 1533–1546 (2022)

[10] Karimi, D., Dou, H., Warfield, S.K., Gholipour, A.: Deep learning with noisy labels: Exploring techniques and remedies in medical image analysis. Medical image analysis **65**, 101759 (2020)

[11] Khanal, B., Shrestha, P., Amgain, S., Khanal, B., Bhattarai, B., Linte, C.A.: Investigating the robustness of vision transformers against label noise in medical image classification. arXiv preprint arXiv:2402.16734 (2024)

[12] Landman, J., Mathur, N., Li, Y.Y., Strahm, M., Kazdaghli, S., Prakash, A., Kerenidis, I.: Quantum methods for neural networks and application to medical image classification. Quantum **6**, 881 (2022)

[13] Lee, K.H., He, X., Zhang, L., Yang, L.: Cleannet: Transfer learning for scalable image classifier training with label noise. In: Proceedings of the IEEE conference on computer vision and pattern recognition. pp. 5447–5456 (2018)

[14] Liu, J., Lim, K.H., Wood, K.L., Huang, W., Guo, C., Huang, H.L.: Hybrid quantum-classical convolutional neural networks. Science China Physics, Mechanics & Astronomy **64**(9), 290311 (2021)

[15] Mathur, N., Landman, J., Li, Y.Y., Strahm, M., Kazdaghli, S., Prakash, A., Kerenidis, I.: Medical image classification via quantum neural networks. arXiv preprint arXiv:2109.01831 (2021)

[16] Mazher, M., Qayyum, A., Khan, M.A., Niederer, S., Mokayef, M., Hassan, C.: Hybrid classical and quantum deep learning models for medical image classification (2024)

[17] Northcutt, C.G., Wu, T., Chuang, I.L.: Learning with confident examples: Rank pruning for robust classification with noisy labels. arXiv preprint arXiv:1705.01936 (2017)

[18] Ostyakov, P., Logacheva, E., Suvorov, R., Aliev, V., Sterkin, G., Khomenko, O., Nikolenko, S.I.: Label denoising with large ensembles of heterogeneous neural networks. In: Proceedings of the European Conference on Computer Vision (ECCV) Workshops. pp. 0–0 (2018)

[19] Shu, J., Xie, Q., Yi, L., Zhao, Q., Zhou, S., Xu, Z., Meng, D.: Meta-weight-net: Learning an explicit mapping for sample weighting. Advances in neural information processing systems **32** (2019)

[20] Trochun, Y., Stirenko, S., Rokovyi, O., Alienin, O., Pavlov, E., Gordienko, Y.: Hybrid classic-quantum neural networks for image classification. In: 2021 11th IEEE International Conference on Intelligent Data Acquisition and Advanced Computing Systems: Technology and Applications (IDAACS). vol. 2, pp. 968–972. IEEE (2021)

[21] Veit, A., Alldrin, N., Chechik, G., Krasin, I., Gupta, A., Belongie, S.: Learning from noisy large-scale datasets with minimal supervision. In: Proceedings of the IEEE conference on computer vision and pattern recognition. pp. 839–847 (2017)

[22] Xue, C., Yu, L., Chen, P., Dou, Q., Heng, P.A.: Robust medical image classification from noisy labeled data with global and local representation guided co-training. IEEE transactions on medical imaging **41**(6), 1371–1382 (2022)

[23] Yang, J., Shi, R., Wei, D., Liu, Z., Zhao, L., Ke, B., Pfister, H., Ni, B.: Medmnist v2-a large-scale lightweight benchmark for 2d and 3d biomedical image classification. Scientific Data **10**(1), 41 (2023)

[24] Yousif, M., Al-Khateeb, B., Garcia-Zapirain, B.: A new quantum circuits of quantum convolutional neural network for x-ray images classification. IEEE Access (2024)

[25] Zhuang, J., Al Hasan, M.: Defending graph convolutional networks against dynamic graph perturbations via bayesian self-supervision. In: Proceedings of the AAAI Conference on Artificial Intelligence. vol. 36, pp. 4405–4413 (2022)

[26] Zhuang, J., Guan, C.: Large language models can help mitigate barren plateaus. arXiv preprint arXiv:2502.13166 (2025)